Initiation of nanosecond electrical breakdown in liquid water: Electron multiplication in long nanocavities

Petr Bílek[1,2], Ján Tungli[2], Zdeněk Bonaventura[2], Milan Šimek[1]

[1]*Department of Pulse Plasma Systems, Institute of Plasma Physics, Czech Academy of Sciences, Prague, Czech Republic.*

[2]*Department of Physical Electronics, MU, Brno, Czech Republic.*

The nanosecond electrical breakdown in liquid water requires a sharp electrode with a radius of tens of micrometers and a voltage pulse having nanosecond rise-time and the magnitude of tens or hundreds of kilovolts [1]. The two most probable driving mechanisms behind the discharge onset are: the field-emission of electrons at the liquid or at metal-liquid interface [2, 3] and the formation of low-density regions [4, 5] due to the electrostriction.

Recently, we proposed that electron multiplication proceeds via a bouncing-like motion of electrons along the stretched cylindrical cavity, where the electrons are freely accelerated due to the applied electric field [6]. This multiplication is sustained by the emission of the secondary electrons from the surface of the cavity.

In this work, we investigate an elementary step of the multiplication process in long cavities, which we define as a propagation of a primary electron released uniformly in the cavity in the presence of the electric field. We derive the distribution function of the electron incidence on the cylinder surface, and we reconstruct the function describing secondary electron yield due to the primary electron impact.

Electron trajectory in a cylindrical cavity with homogeneous electric field is described using spherical coordinates:

$$x = v_0 t \sin\theta\cos\phi, \qquad y = v_0 t \sin\theta\sin\phi, \qquad z = v_0 t\cos\theta + \frac{qE}{2m_\mathrm{e}}t^2, \tag{1}$$

where v_0 is the initial velocity of the electron, t is the time elapsed from the instant of electron release and E is the applied electric field. Electron is released from the origin of the coordinate system and vector of the initial velocity v_0 is defined using two angles θ and ϕ, where $\theta \in (0,\pi)$ and $\phi \in (-\frac{\pi}{2},\frac{\pi}{2})$, see figure 1. Electron time of flight until hitting the cylinder surface is $t_\mathrm{fl} = \frac{2R\cos\phi}{v_0\sin\theta}$ and the z-coordinate of hitting point is:

$$\frac{z}{R} = v_0\cos\theta\ \left(\frac{t_\mathrm{fl}}{R}\right) + \frac{q}{2m_\mathrm{e}}(E\cdot R)\ \left(\frac{t_\mathrm{fl}}{R}\right)^2 = l\cot\theta + \frac{Al^2}{2}(\cot^2\theta + 1), \tag{2}$$

where we modified the equation, setting $A = \frac{qER}{m_\mathrm{e}{v_0}^2}$ and $l = 2\cos\phi$.

Our goal is to obtain a non-trivial distribution of the electron incidence probability as a function

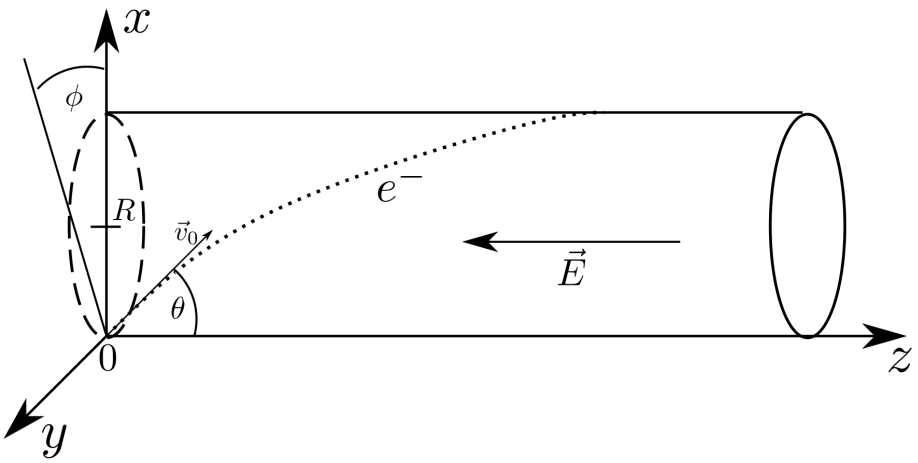

Figure 1: Coordinate system used for the description of electron motion within the cylindrical cavity. The motion is reduced only to the plane perpendicular to $x-y$ plane, that includes $\vec{v}_0$.

of ϕ and z/R. We suppose that the velocity of the released electron is uniformly distributed on a hemisphere, which top is located in the x-axis direction. Using substitutions $\frac{z}{R} = Z$ and $\cot\theta = \xi(Z)$ to the equation (2), we arrive to the quadratic equation:

$$\frac{Al^2}{2}\xi^2 + l\xi + \frac{Al^2}{2} - Z = 0. \tag{3}$$

Its quadratic form implies that a point in the cylinder can be hit in two ways, first is the electron released with the z-velocity component along the electric field and the second against the electric-field direction. The solution of the equation (3) is:

$$\xi_\pm = -\frac{1}{Al} \pm \sqrt{-1 + \frac{1+2AZ}{(Al)^2}}, \tag{4}$$

indicating that some regions, those with $Z < \frac{(Al)^2-1}{2A}$, in the cylinder will not be hit at all.
It can be shown (transforming the condition for the uniform release $\frac{1}{\pi}\int_0^{\frac{\pi}{2}}\int_0^{\pi}\sin\theta\,\mathrm{d}\theta\,\mathrm{d}\phi = 1$) that the distribution of electron incidence probability in the prefered variables $(\phi; Z)$ is:

$$P(Z,\phi) = \left[\frac{1}{(1+\xi_+^2)^{\frac{3}{2}}} + \frac{1}{(1+\xi_-^2)^{\frac{3}{2}}}\right] \cdot \left|\frac{\mathrm{d}\xi}{\mathrm{d}Z}\right|, \qquad \text{where} \qquad \frac{\mathrm{d}\xi_\pm}{\mathrm{d}Z} = \frac{\pm 1}{Al^2\sqrt{-1+\frac{1+2AZ}{(Al)^2}}} \tag{5}$$

and ξ in $P(Z,\phi)$ being expressed as the function of Z. The new transformation also meets the normalization condition; however, Z has to be varied within new limits, defined by the points of the cylinder surface, which can be hit:

$$\frac{1}{\pi}\int_0^{\frac{\pi}{2}}\int_{Z_{\min}}^{\infty} P(Z,\phi)\,\mathrm{d}Z\,\mathrm{d}\phi = 1, \qquad \text{where} \qquad Z_{\min}(\phi) = \frac{(2A\cos\phi)^2 - 1}{2A}. \tag{6}$$

The distributions of electron incidence plotted for four different $E \cdot R \in [10, 15, 20, 25]$ eV and the initial energy of the electron $\varepsilon_0 = \frac{1}{2} m_e v_0^2 = 7.4$ eV are shown in the figure 2. The shift of the distribution towards the higher z/R with the increasing $E \cdot R$ is observed. Note that the electron is released from $(\phi = \frac{\pi}{2}; Z = 0)$.

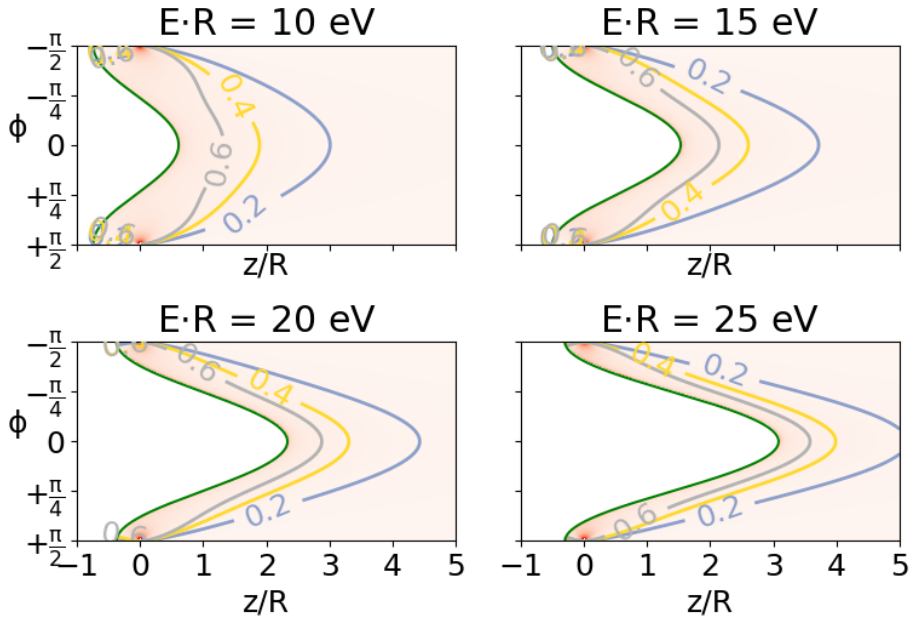

Figure 2: The distributions of electron incidence probability plotted for $E \cdot R$ = 10, 15, 20 and 25 eV. The green curve, given by $Z_{\min}(\phi)$, denotes the limit boundary for possible electron impact.

Whether the incident electron causes the emission of the secondary electrons depends on its incident energy ε and the angle of incidence ψ. These two parameters are expressed as:

$$\varepsilon = \varepsilon_0 + \frac{z}{R}(E \cdot R) \qquad \text{and} \qquad cos\psi = \sqrt{\frac{\varepsilon_0}{\varepsilon}} \sin\theta \cos\phi . \tag{7}$$

The set of (ε, ψ) values predicate the number of secondary electrons released back to the cavity, and this number $S(\varepsilon, \psi)$ is defined in the figure 12(a) of [6]. For positions in the cavity, where $z/R > Z_{\min}(\phi)$, the number of secondary electrons $S(\varepsilon(z/R), \psi(z/R, \phi))$ is plotted in figure 3(a). This is again done for $E \cdot R \in [10, 15, 20, 25]$ eV and $\varepsilon_0 = 7.4$ eV. It is apparent that the threshold ($S(\varepsilon, \psi) = 1$) ensuring electron gain is reached only for higher z/R, for example, $z/R \sim 8$ for $E \cdot R = 20$ eV. However, such high values of z/R imply just a small incidence probability (see figure 2). We conclude that there has to be very important influence of primary-electron bouncing, which virtually enhances the gain of secondary electrons. Indeed, after summing the

number of secondary electrons $S(\varepsilon(z/R),\ \psi(z/R,\phi))$ with the probability of primary electron bouncing $P(\varepsilon(z/R),\ \psi(z/R,\phi))$ as shown in the figures 12(a) and 12(b) of [6], we obtain much greater values for the total electron gain, see the figure 3(b). Moreover, the electron gain for the $E \cdot R = 20$ eV reaches the threshold ($S(\varepsilon,\ \psi) = 1$) already at $z/R \sim 2$, which is the distance having high electron incidence probability.

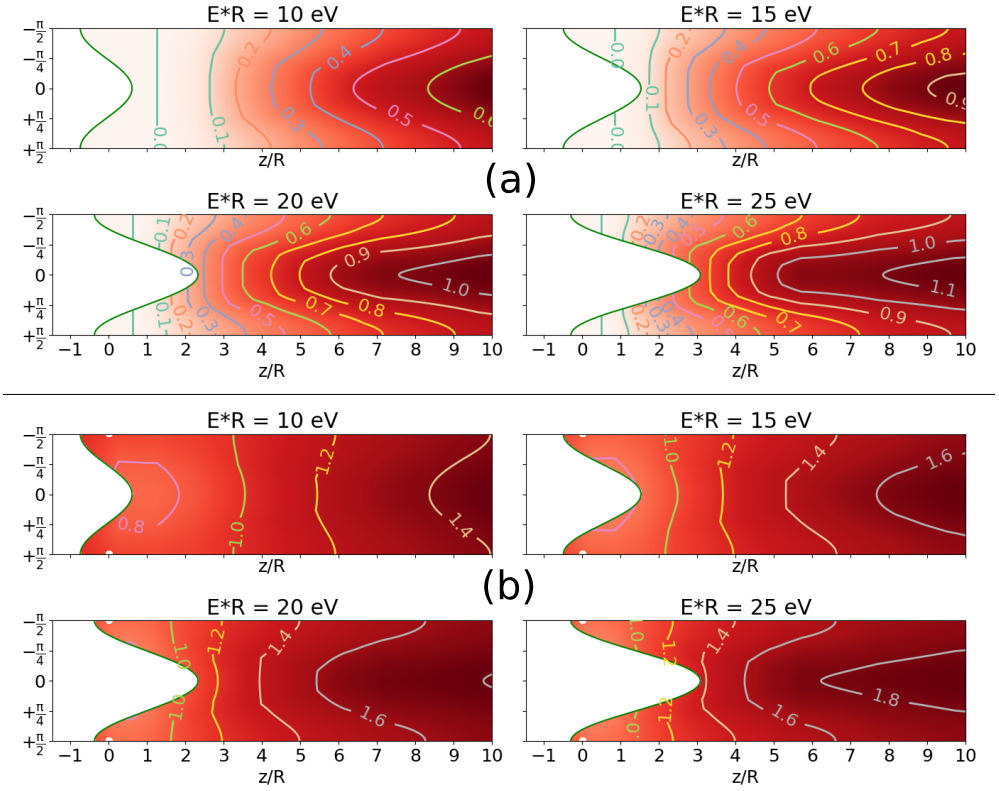

Figure 3: (a) The number of secondary electrons released back to the cavity. (b) The total number of electrons released back to the cavity (including bouncing of the primary electron).

In conclusion, we showed that the bouncing of primary electron on the void-liquid interface is important to maintain the electron multiplication for the investigated $E \cdot R$ range. The results of this work clarify important details behind the efficient process of electron multiplication in long cavities. **This contribution is funded by the Czech Science Foundation grant no. 18-04676S.**

References

[1] M. Šimek et al., Plasma Sources Science and Technology, **29** (6) (2020).

[2] A. C. Aghdam and T. Farouk, Plasma Sources Science and Technology, **29** (2) (2020).

[3] K. Grosse et al., Plasma Sources Science and Technology, **29** (9) (2020).

[4] Y. Li et al., Plasma Sources Science and Technology, **29** (7) (2020).

[5] X. Zhang and M. N. Shneider, Journal of Applied Physics, **129** (10) (2021).

[6] Z. Bonaventura et al., Plasma Sources Science and Technology, (2021).